Spectral Characterization of Eucalyptus Wood

CARMEN-MIHAELA POPESCU,* MARIA-CRISTINA POPESCU, GHITA SINGUREL, CORNELIA VASILE, DIMITRIS S. ARGYROPOULOS, and STEFAN WILLFOR

Romanian Academy "P.Poni" Institute of Macromolecular Chemistry, 41A Gr. Ghica Voda Alley, Ro.700487, IASI, Romania (C.-M.P., M.-C.P., C.V.); "Al. I.Cuza" University, Faculty of Physics, Optics and Spectroscopy Department, 11 Blvd. Carol I, Iaşi, Romania (G.S.); Forest Biomaterials Laboratory College of Natural Resources North Carolina State University (D.S.A.); and Process Chemistry Centre, Abo Akademi University, Finland (S.W.)

The main difficulties in wood and pulp analyses arise principally from their numerous components with different chemical structures. Therefore, the basic problem in a specific analytical procedure may be the selective separation of the main carbohydrate-derived components from lignin due to their chemical association and structural coexistence. The processing of the wood determines some structural modification in its components depending on the type of wood and the applied procedure. Fourier transform infrared (FT-IR) spectrometry and X-ray diffraction have been applied to analyze *Eucalyptus g.* wood chips and unbleached and chlorite-bleached pulp. The differences between samples have been established by examination of the spectra of the fractions obtained by successive extraction (acetone extractives, acetone free extractive samples, hemicelluloses, and lignins) by evaluating the derivative spectra, band deconvolution, etc. The energy and the hydrogen bonding distance have been evaluated. The relationship between spectral characteristics and sample composition has been established, as well as the variation of the degree of crystallinity after pulping and bleaching. The integral absorption and lignin/carbohydrate ratios calculated from FT-IR spectra of the IR bands assigned to different bending or stretching in lignin groups are stronger in the spectrum of eucalyptus chips than those from brown stock (BS) pulp spectra because of the smaller total amount of lignin in the latter. FT-IR spectra clearly show that after chlorite bleaching the structure of the wood components is partially modified or removed. Along with FT-IR data, the X-ray results confirmed the low content of lignin in the pulp samples by increasing the calculated values of the crystalline parameters. It was concluded that FT-IR spectroscopy can be used as a quick method to differentiate *Eucalyptus globulus* samples.

Index Headings: **Wood components; Fourier transform infrared spectroscopy; FT-IR spectroscopy; X-ray diffraction; XRDS.**

INTRODUCTION

Wood remains one of our most important renewable natural polymers, providing shelter, supporting transportation, and even allowing us to effectively communicate via writing.[1] Wood consists of an orderly arrangement of cells with walls composed of varying amounts of cellulose, hemicelluloses, and lignin. The great diversity of woody plants is reflected in their varied morphology and chemical composition.

Cellulose is an optically anisotropic system made up of poly-β(1→4)-β-D-glucose chains. On first sight, the molecular structure gives the impression of being very simple, but in fact the structural characteristics of the molecule have not yet been fully resolved.[2,3] The numerous strongly polar groups make cellulose molecules predestined for building up hydrogen bonds within the molecule and between the different molecules. In the generally accepted structure of cellulose I, intramolecular hydrogen bonds of types 3-OH···O-5 and 2-OH···O-6 are present for both sides of the chain.[4] As a result of hydroxyl groups showing different polarities, cellulose has different crystalline structures, ranging from cellulose I (native cellulose) to cellulose IV. Moreover, cellulose I is itself composed of two different crystalline forms: cellulose Iα and Iβ.[5] From crystallographic studies, it has been concluded that the secondary structure of native cellulose is a ribbon-like conformation with an approximately two-fold helical structure.[3] Two chains, which take an almost fully extended conformation, are contained in the unit cell of cellulose I. The cellulose molecule chain itself is not very stiff, but rather semi-flexible. It is generally known and accepted that the hydrogen bonds play an important role in the conformational and mechanical properties of cellulosic materials.[2] Besides its complex crystalline structure, native cellulose also has a complex arrangement within the wood fiber wall. In the secondary wall, the cellulose chains are grouped into fibrils by hydrogen bonds. These fibrils are aligned in different directions in the secondary wall layers. Such complexities in fibril alignment are what render wood pulp fibers used in paper sheets into a much more complicated material compared to other materials, such as synthetic polymers.

Infrared spectroscopy, which is known to be sensitive to structural features, is a technique routinely used by chemists, biochemists, and material scientists as a molecular probe. It has had a long tradition in wood, pulp, cellulose, and lignin research. The observed spectroscopic signals are due to the absorption of infrared radiation that is specific to functional groups of the molecule. The absorption frequencies are associated with the vibrational motions of the nuclei of a functional group and show distinct changes when the chemical environment of the functional group is modified. It is extremely rapid and is a nondestructive and noninvasive method for analyzing the structure of wood constituents[6] and the chemical and structural changes taking place in wood components due to different treatments (natural or artificial aging,[7] oxidation,[8] thermal degradation,[9] etc.). Infrared spectroscopy also has the ability to probe interactions between macromolecules.[10]

The first use of infrared spectroscopy was to elucidate molecular structures, but some efforts have been devoted to separating the overlapping bands deriving, for example, from hydrogen bonds.[4,11–18]

Wada et al.[19] carried out an X-ray least squares refinement program to differentiate several cellulose samples into two categories: one coincided with Iα (algal–bacterial type) rich in the triclinic phase, the other with Iβ (cotton–ramie type) rich in the monoclinic phase.

Principally, the difficulties in wood and pulp analyses arise from the numerous components with different chemical characters. The extractive samples of wood and pulp cover a wide range of low-molecular-mass chemical compounds, which may be isolated for a detailed chemical examination

Received 23 March 2007; accepted 6 August 2007.

* Author to whom correspondence should be sent. E-mail: mihapop@icmpp.ro.

0003-7028/07/6111-1168$2.00/0

TABLE I. Average contents of total extractives, carbohydrates, and lignin in *Eucalyptus globulus* samples.

Samples	Extractives[a] (%)	Carbohydrates[b] (%)	Lignin[c] (%)
Eucalyptus chips	1.06–2.98	57.1–70.6	24.5–27.6
Eucalyptus BSP[d]	0.14–2.16	88.7–99.2	1.0–1.7

[a] Total amount of extractives determined by extraction in different solvents.[20]
[b] Total amount of carbohydrates determined by high-performance anion-exchange chromatography with pulsed amperometric detection (HPAEC-PAD).[21]
[c] Total amount of lignin (ASL+AIL).[22]
[d] BSP: brown stock pulp.

by means of different solvent extraction techniques. The isolation of lignin from wood and pulp samples in its unaltered form with an acceptable yield is currently a major problem, although a number of versatile extraction schemes have been suggested. Determination of the carbohydrate composition of wood and pulp samples is vital for many applications and is one of the most frequently performed chemical analyses for almost all biomass-derived materials.

This paper deals with the study of the structural and morphological changes of eucalyptus wood samples in order to elucidate the molecular basis of differences found between them after different treatments. Fourier transform infrared (FT-IR) spectrometry and X-ray diffraction are used. Optimal experimental conditions have been established for each investigation method and differences between samples have been assessed by determination of the characteristic bands, integral absorption, or carbohydrate/lignin ratio from FT-IR spectra and the percentage of crystalline fraction by X-ray diffraction, etc., and their dependence on the samples' composition is discussed.

EXPERIMENTAL DETAILS

The unfractionated samples of wood chips of *Eucalyptus globulus* from the same batch as the pulp, unbleached Kraft pulp brown stock (BS) of *Eucalyptus globulus* (sampled after the washing stages) were provided by Abo Akademi University, Laboratory of Wood and Paper Chemistry, Turku, Finland, and chlorite-bleached Kraft pulp brown stock of *Eucalyptus globulus* was prepared by AFOCEL, France. All samples are from the COST E41 joint analysis effort.

Different working groups (WG1, WG2, and WG3 consisting of different laboratory partners) of the COST Action E41 Project determined the composition of the wood components following different separation procedures. The results were summarized at the Grenoble Meeting (12–13 April, 2006). The average contents of the components are presented in Table I.

The chlorite-bleached Kraft pulp brown stock resulted from Kraft pulp brown stock; its changes in composition and structure will be established in this study. The studied samples have very different contents with regard to extractives, carbohydrates, and lignins.

The methods of investigation in this work were FT-IR spectrometry and X-ray diffraction (XRD) spectroscopy.

Fourier Transform Infrared Spectra. Fourier transform infrared spectra were recorded on solid samples in KBr pellet form by means of a Bomem MB-104 Fourier transform spectrometer equipped with a deuterated triglycine sulfide (DTGS) detector and Zn/Se optics. Data collection was performed with a 4 cm^{-1} spectral resolution and 60 scans were taken per sample. The concentration of the samples in the pellets was constant (5 mg/500 mg KBr). Dust samples were sieved and the fraction with a diameter less than 0.2 mm was retained for analysis. Five recordings were performed for each sample after successive milling and the evaluations were made on the average spectrum obtained from these five recordings. Processing of the spectra was done by means of the Grams/32 software (Galactic Industry Corp.). For a better understanding of the structure of the samples, deconvolution of the spectra was carried out with Gaussian contours. The number and the maximum of the deconvoluted peaks were taken from second-derivative spectra. The reduced chi-squared value for all the deconvoluted curves was $\chi^2 \leq 0.1$; therefore, the use of this function is a good approach.

X-ray Diffractograms. The X-ray diffractograms were recorded on XRD equipment Rigaku RINT 2500/32 from Rigaku Co. Japan. This device was used to determine the crystallinity of the cellulose. The measurements were carried out in point focus geometry using Cu K_α radiation, $\lambda = 0.1524$ nm. Experimental conditions were as follows: sequence scan mode; measuring axis: 2θ; voltage: 40 kV; current: 20 mA; start angle: 10°; stop angle: 80°; sampling angle: 0.021°; scan rate of goniometer: 2°/min; divergent slit width: 1°; receiving slit width: 1°; scattering slit width: 0.60 mm; and monochromator receiving slit width: 0.80 mm. All the measurements were conducted in diffraction mode in air atmosphere (pressure).

The diffractograms were deconvoluted using Gaussian and mixed Gaussian–Lorentzian profiles. The reduced chi-squared value for all the deconvoluted curves was $\chi^2 \leq 0.1$; therefore, the use of this function is a good approach. The fitting curve matches the experimental curve very well. After deconvolution, several parameters can be calculated and compared,[23–25] e.g., the crystalline index, proposed by Hermans.[25]

$$\text{Cr.I.} = \frac{A_{\text{cryst}}}{A_{\text{total}}} \tag{1}$$

where Cr.I. is the crystalline index, A_{cryst} is the sum of the peak areas (101), (10$\bar{1}$), (002), and (012), and A_{total} is the total area under the diffractogram. Vuorinen and Visapä[26] and Segal used intensity data:

$$\text{Cr.I.}' = 1 - \frac{I_{\text{am}}}{I_{002}} \tag{2}$$

where I_{002} is the maximum intensity of the (002) lattice diffraction, and I_{am} is the intensity diffraction of the amorphous band. The apparent crystallite size was estimated through the use of the Scherrer equation:[6,7,23–28]

$$L = \frac{K\lambda}{\beta \cos\theta} \tag{3}$$

where K is a constant with a value of 0.94, λ is the X-ray wavelength (0.1542 nm for Cu K_α radiation), β is the half-height width of the diffraction peak, and θ is the Bragg angle corresponding to the (002) plane. The surface chains occupy a layer approximately 0.57 nm thick, so the proportion of crystallite interior chains is:[6]

$$X = \frac{(L - 1.14)^2}{L^2} \tag{4}$$

where L is the apparent crystallite size for the (002) reflection. The orientation index was estimated using the equation[24]

$$\text{O.I.} = \left(1 - \frac{I_{\text{am}}}{I_{\text{tot}}}\right) \quad (5)$$

where I_{tot} is the maximum intensity of the diffraction pattern. Mesomorphism was calculated according to:[24]

$$\text{Mm} = (\text{O.I.} - \text{Cr.I.}) \quad (6)$$

The mass fraction of cellulose in wood may be estimated using the crystallinities of wood and cellulose:

$$\text{cell.content} = \frac{\text{Cr.I.}'}{\text{Cr.I.}_{\text{cell}}} \quad (7)$$

where $\text{Cr.I.}_{\text{cell}} = 70\%$.[29]

RESULTS AND DISCUSSION

Fourier Transform Infrared Spectroscopy. Fourier transform infrared spectroscopy is often used to characterize wood[6,28] and to determine cellulose or lignin content in pulp, paper, and wood. It has also been used for determination of chemical changes in wood during weathering, fungal decay,[30] and chemical treatments,[7] and its use was recently reviewed by Moore and Owen.[31] Two information-rich regions of the FT-IR spectra of the studied samples are shown in Figs. 1A and 1B.

The spectra of the samples are particular to each sample. The main bands are assigned to asymmetric methoxyl C–H stretching at 2921 cm^{-1}, absorbed water at 1640 cm^{-1}, bands assigned to different lignin groups, such as those at 1770, 1740, 1590, 1510, 1270, and 1140 cm^{-1}; bands common to lignin and cellulose such as those at 1460, 1420, 1375, 1330, 1230, 1160, 1110, and 1030 cm^{-1}; and bands assigned to cellulose such as those at 1315, 1280, 1180, and 1060 cm^{-1}. In the "fingerprint region" there are easily observed differences between the studied samples that distinguish them from normal spectra (see also Table II). Some bands in pulp samples that are assigned to lignin were not found (1770 and 1740 cm^{-1}) or the integral absorptions are very low (1590, 1510, and 1270 cm^{-1}). For a good differentiation of the bands, the second derivative of the spectra was made.

Generally, the second derivatives of IR spectra can obviously enhance the apparent resolution and amplify small differences in the IR spectra. These were obtained with the Savitzky–Golay method (second-order polynomial with fifteen data points) using the Grams 32 software. The second-derivative spectra of the samples are shown in Fig. 2.

From the second-derivative FT-IR spectra of the samples several differences can be observed. The bands at 1737, 1665, 1596, 1510, and 1463 cm^{-1} decrease in pulp samples, while the bands at 1270, 1238, 1210, 1062, and 1030 cm^{-1}, which in the chip sample appear as broad bands, become more prominent and are better evidenced in pulp samples.

Also, for a good interpretation of the infrared spectra and for determining the integral absorption and the height of each band, the deconvolutions of the 3800–2750 cm^{-1}, 1850–1550 cm^{-1}, 1550–1250 cm^{-1}, and 1250–900 cm^{-1} regions were carried out for all samples. The reduced chi-squared value for all the deconvoluted curves was $\chi^2 \leq 0.1$, confirming the use of this function. In Figs. 3A–3D are presented the deconvolutions of the eucalyptus chip sample.

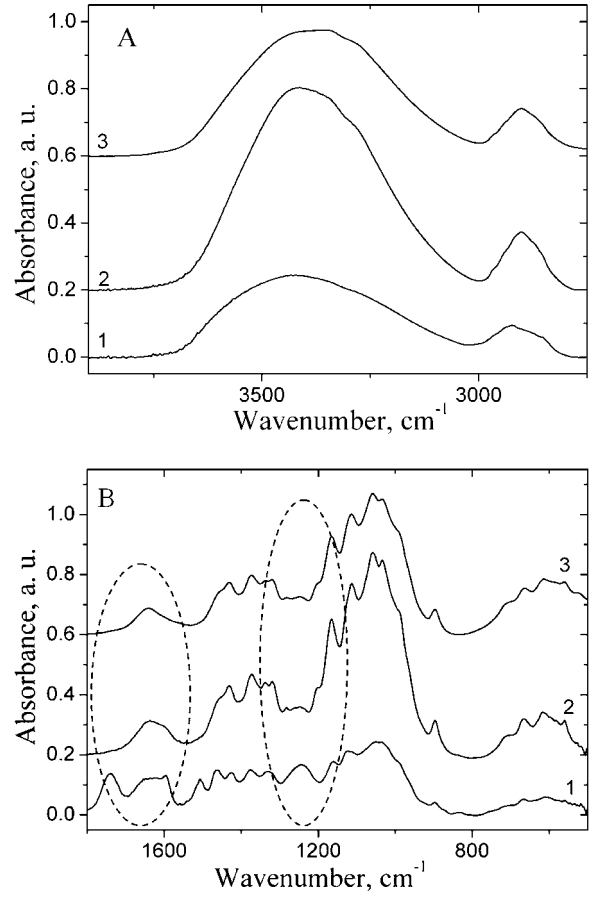

FIG. 1. FT-IR spectra of (**A**) the 3700–2700 cm^{-1} region and (**B**) the 1850–500 cm^{-1} region from unfractioned wood samples: (***1***) eucalyptus chips, (***2***) eucalyptus brown stock pulp, and (***3***) eucalyptus chlorite-bleached pulp.

The 3800–2750 cm^{-1} region (Figs. 3A and 3B) contains seven bands at 3567, 3423, 3342, 3278, 3106, 2921, and 2851 cm^{-1}. The assignments of these bands are presented in Table II.

The "fingerprint" region from 1800 to 800 cm^{-1} (Figs. 3C–3H) is very complicated. It comprises twenty-seven bands, some of which are evidenced only by deconvolutions. These bands are assigned to the main components from wood: cellulose, hemicelluloses, and lignin (see Table II).

The deconvoluted spectra in all studied regions are different between the eucalyptus chip sample and the unbleached and chlorite-bleached brown stock pulp samples. Generally in the unbleached and chlorite-bleached brown stock pulp spectra the bands assigned to lignin are very low (1590, 1510, 1270, 1240, and 1210 cm^{-1}) or are even missing (1770 and 1740 cm^{-1}).

The band at 1770 cm^{-1} in eucalyptus chips, where the content of lignin in the sample is ~27 wt %, is very low, and in the unbleached and chlorite-bleached BS pulp samples, where the content of lignin is ~1.5 wt %, the band at 1770 cm^{-1} is missing. The band at 1740 cm^{-1} is easily observable in the spectra of eucalyptus chips, while in the pulp samples the band is missing. This is in accordance with the results of chemical analysis (see Table I); therefore, these bands can be used for lignin determination.

Generally, the integral absorption and the height of the lignin-assigned bands in FT-IR spectra of the pulp samples decreases or are even missing, while the bands assigned to cellulose are higher than those presented in the eucalyptus chip

TABLE II. The characteristic bands in FT-IR spectra of the studied samples and their assignments according to the literature data.

Wavenumber (cm^{-1})	Band assignment[c]	Eucalyptus chips	Eucalyptus BSP[a]	Eucalyptus CBP[b]
3580–3550	Free OH(6) and OH(2), weakly absorbed water[35–37]	3568	3561	3557
3460–3405	O(2)H. . .O(6) intramolecular hydrogen bonds[11,32,34,35]	3423	3419	3421
3375–3340	O(3)H. . .O(5) intramolecular hydrogen bonds in cellulose[32,34,38]	3342	3344	3342
3310–3230	O(6)H. . .O(3) intermolecular hydrogen bonds in cellulose[4,17,12,34,35]	3278	3277	3271
3175	–OH stretching intramolecular hydrogen bonds in cellulose II[34,38]	3106	3111	3106
2938–2920	Symmetric CH stretching in aromatic methoxyl groups and in methyl and methylene groups of side chains[32,34,38]	2921	2916	2911
2840–2835	Asymmetric CH stretching in aromatic methoxyl groups and in methyl and methylene groups of side chains[32,34,38]	2852	2854	2852
1770–1760	C=O stretching in conjugated ketones[28,32–34]	1757	—	—
1740–1720	C=O stretch in unconjugated ketones[28,32–34]	1740	—	—
1650–1640	Water associated with lignin or cellulose[32,34]	1647	1637	1641
1610–1590	C=C stretching of the aromatic ring (S)[32,34]	1593	1594	1596
1515–1505	C=C stretching of the aromatic ring (G)[32–34]	1508	1510	1510
1470–1455	C–H asymmetric deformation in $–OCH_3$, CH_2 in pyran ring symmetric scissoring[32–34,38]	1463	1455	1454
1430–1422	C–H asymmetric deformation in $–OCH_3$[32–34,38]	1426	1427	1427
1375–1365	CH bending in cellulose I and cellulose II and hemicellulose[32–34,38]	1376	1373	1373
1335–1320	C_1–O vibrations in S derivatives, CH in-plane bending in cellulose I and cellulose II[28,32–34,38]	1331	1338	1337
1315	CH_2 wagging in cellulose I and cellulose II[34,38]	1315	1317	1316
1282–1277	CH deformation in cellulose I and cellulose II[34]	—	1283	1282
1268	Guaiacyl ring breathing, C–O linkage in guaiacyl aromatic methoxyl groups[32,34]	1259	1263	1259
1235–1230	Syringyl ring breathing and C–O stretching in lignin and xylan[32–34]	1231	1234	1234
1205–1200	OH in-plane bending in cellulose I and cellulose II[34]	1205	1203	1203
1162–1125	C–O–C asymmetric stretching in cellulose I and cellulose II[32–34,38]	1162	1166	1166
1140	Aromatic C–H in-plane deformation; typical for G units, where G condensed > G etherified[32,34]	1127	1130	1128
1128–1110	Aromatic C–H in-plane deformation (typical for S units), C=O stretch[32–34]	1108	1111	1113
1086–1075	C–O deformation in secondary alcohols and aliphatic ethers[34]	1081	1079	
1060–1015	C–O valence vibration mainly from C(3)–O(3)H[32,34,38]	1056	1060	1060
1047–1004	C–O stretching in cellulose I and cellulose II[32–34,38]	1034	1029	1027
996–985	C–O valence vibration[34]	988	987	994
970	=CH out-of-plane deformation (*trans*)[34]	959	961	957
930–915	Aromatic C–H out-of-plane deformations, pyran ring vibration[34]	932	928	933

[a] BSP: brown stock pulp.
[b] CBP: chlorite-bleached pulp.
[c] S: syringyl; G: guaiacyl.

sample. Also, the positions of the band maxima vary in close limits for eucalyptus chips and pulp samples.

The most representative bands in the 3700–2700 cm^{-1} region are those assigned to OH intramolecular and intermolecular stretching modes (3567, 3423, 3342, 3278, and 3106 cm^{-1}) and to asymmetric and symmetric methyl and methylene stretching (2921 and 2854 cm^{-1}) in all components of wood.

In the 3800–2750 cm^{-1} region, four bands assigned to different hydrogen bonded OH vibrations were found. The energy of hydrogen bonds and the hydrogen bonding distance were calculated for these bands.

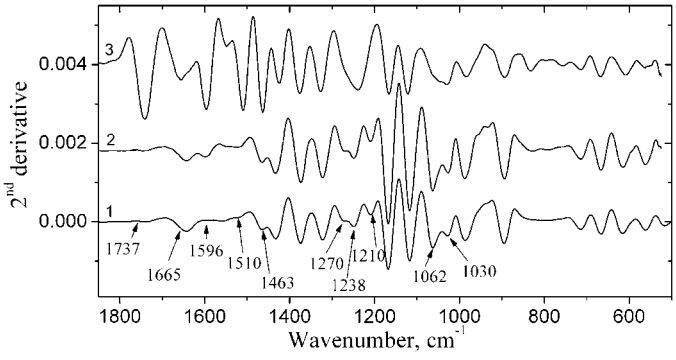

FIG. 2. Second-derivatives of FT-IR spectra in the "fingerprint" region (1850–900 cm^{-1}) for: (*1*) eucalyptus chlorite-bleached pulp, (*2*) eucalyptus brown stock pulp, and (*3*) eucalyptus chips.

The positions of the 3568, 3423, and 3278 cm^{-1} bands are shifted to lower wavenumbers after pulping treatment, while the band at 3342 cm^{-1} remains approximately constant, indicating changes in the relationship between components because of both composition modification and ordering of chains (crystallinity increase; see Table V below), and as a consequence of intermacromolecular interactions. The band position shift to lower wavenumbers is observed for other bands as well, such as: 2921 to 2911 cm^{-1}, 1647 to 1641 cm^{-1}, 1463 to 1454 cm^{-1}, 1376 to 1363 cm^{-1}, 1331 to 1338 cm^{-1}, 1259 to 1263 cm^{-1}, 1231 to 1234 cm^{-1}, 1162 to 1166 cm^{-1}, 1127 to 1130 cm^{-1}, 1108 to 1111 cm^{-1}, 1081 to 1079 cm^{-1}, 1056 to 1060 cm^{-1}, and 959 to 961 cm^{-1}.

The energy of the hydrogen bonds was calculated using the following formula:[39]

$$E_H = \frac{1}{k}\left[\frac{(\nu_0 - \nu)}{\nu_0}\right] \quad (8)$$

where ν_0 is the standard frequency corresponding to free OH groups (3650 cm^{-1}), ν is the frequency of the bonded OH groups, and k is a constant equal to 2.61×10^2 kJ.

The calculated energy of the hydrogen bonds, shown in Table III, presents a small increase in the series of samples studied; probably the molecules forming weaker bonds are

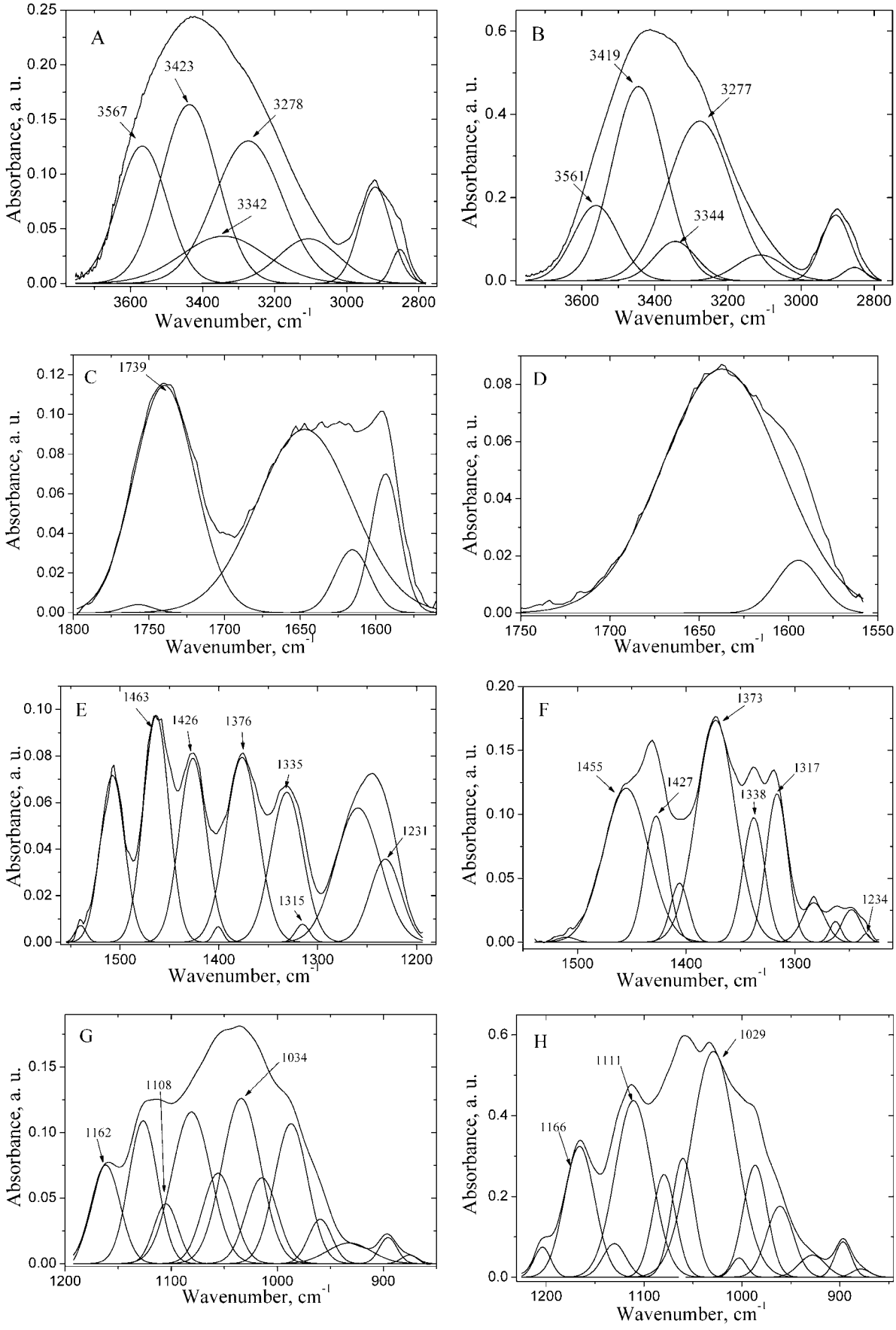

FIG. 3. The deconvoluted spectra of four different spectral regions; (**A**, **B**) 3800–2700 cm^{-1}; (**C**, **D**) 1800–1550 cm^{-1}, (**E**, **F**) 1550–1250 cm^{-1}, and (**G**, **H**) 1250–900 cm^{-1} for eucalyptus chips and unbleached eucalyptus BS pulp samples, respectively.

TABLE III. The energy of the hydrogen bonding for the samples studied.

Samples	Hydrogen bonding energy (E_H)			
	3567 cm^{-1}	3432 cm^{-1}	3342 cm^{-1}	3252 cm^{-1}
Eucalyptus chips	5.86	16.23	21.88	26.60
Eucalyptus BSP[a]	6.39	16.37	22.02	26.67
Eucalyptus CBP[b]	6.65	16.51	22.02	27.10

[a] BSP: brown stock pulp.
[b] CBP: chlorite-bleached pulp.

removed, leaving only those with stronger interactions. Only the energy for the O(3)H...O(5) intramolecular H bonds in cellulose, the stretching modes of intramolecular H bonds, is decreasing in the same series of samples studied. This means that after treatment of wood, the interactions of the O(3)H...O(5) intramolecular H bonds in cellulose molecules are weak. The difference between hydrogen bonds was also evidenced in the synchronous and asynchronous spectra, shown in Fig. 4, from which it can be observed that the band at 3335 cm^{-1} is variable among the samples, while the other bands at 3567, 3421, and 3278 cm^{-1} are unshifted.

The hydrogen bonding distances are obtained by using the Sederholm equation:[40]

$$\Delta\nu(cm^{-1}) = 4.43 \times 10^3(2.84 - R) \quad (9)$$

where $\Delta\nu = \nu_0 - \nu$; ν_0 is the monomeric OH stretching frequency, taken to be 3600 cm^{-1}; and ν is the stretching frequency observed in the infrared spectrum of the sample.[41]

The hydrogen bonding distances, shown in Table IV, are almost constant for certain wavenumbers and show a small decrease after pulping treatment, explaining the increase in the energy of the hydrogen bonding of the processed samples.

In the "fingerprint region" the spectra are very complex, containing many bands assigned to all components of wood. These are found at 1594, 1510, 1268, and 1140 cm^{-1}, assigned to characteristic bending or stretching of different groups from lignin, where the bands centered at 1460, 1420, 1375, 1331, 1230, 1160, 1110, and 1030 cm^{-1} are assigned to the characteristic bending or stretching of different groups commonly for lignin and cellulose, and the bands at 1739, 1315, 1280, 1180, and 1060 cm^{-1} are assigned to the characteristic bending or stretching of different groups from cellulose.

In the spectra of the eucalyptus brown stock unbleached and chlorite-bleached pulp samples there are some bands assigned to characteristic bending or stretching for different lignin groups that are missing (1760 and 1740 cm^{-1}) or are very small

TABLE IV. The hydrogen bonding distance for the samples studied.

Samples	Hydrogen bonding distance (R) (Å)			
	3567 cm^{-1}	3432 cm^{-1}	3342 cm^{-1}	3252 cm^{-1}
Eucalyptus chips	2.833	2.800	2.800	2.781
Eucalyptus BSP[a]	2.831	2.799	2.799	2.782
Eucalyptus CBP[b]	2.830	2.795	2.795	2.782

[a] BSP: brown stock pulp.
[b] CBP: chlorite-bleached pulp.

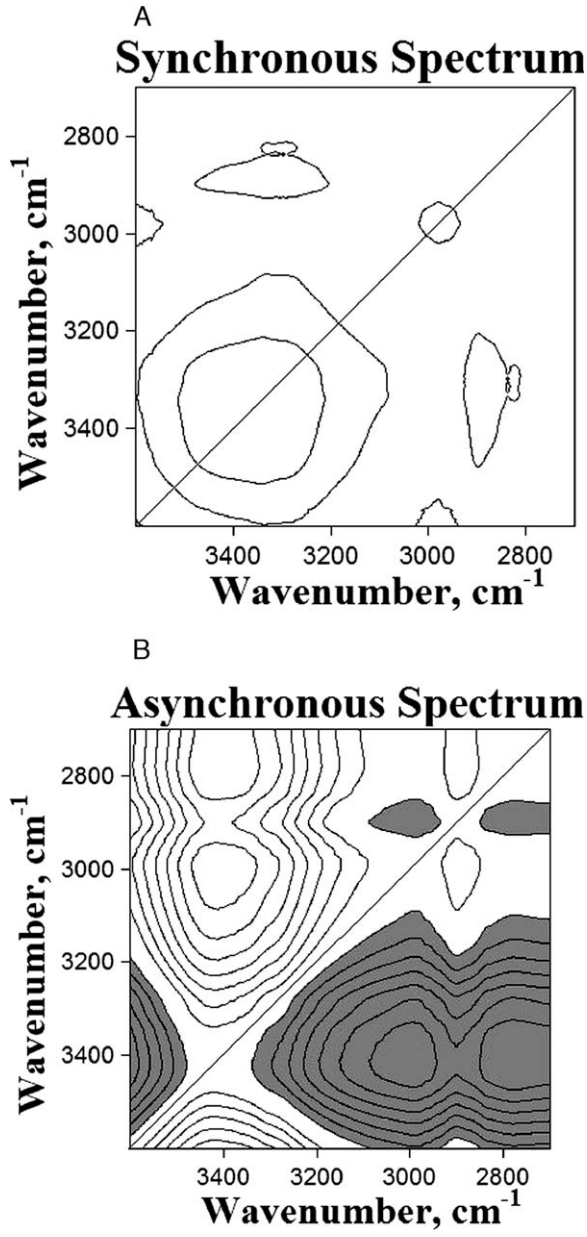

FIG. 4. Synchronous and asynchronous spectra in the 2700–3600 cm^{-1} region of *Eucalyptus globulus* samples.

(1510, 1260, and 1230 cm^{-1}) in comparison with the same bands in the eucalyptus chip sample. This latter group of bands was possible to detect only after carrying out deconvolution. As can be seen in Fig. 5, the integral absorption of the bands assigned to characteristic bending or stretching in lignin groups decreases strongly in the sample series studied. Only for the band at 1140 cm^{-1}, assigned to the aromatic C–H in-plane deformation, typical for G units, where G condensed > G etherified, is the decrease not so rapid. The variation of the integral absorptions of the bands from the IR spectra, assigned to different bending or stretching in lignin groups, are in concordance with the total amount of lignin chemically determined (see Table I).[22] These bands can be used for rapid evaluation of lignin content in the samples.

It seems that the bands assigned to lignin show a small

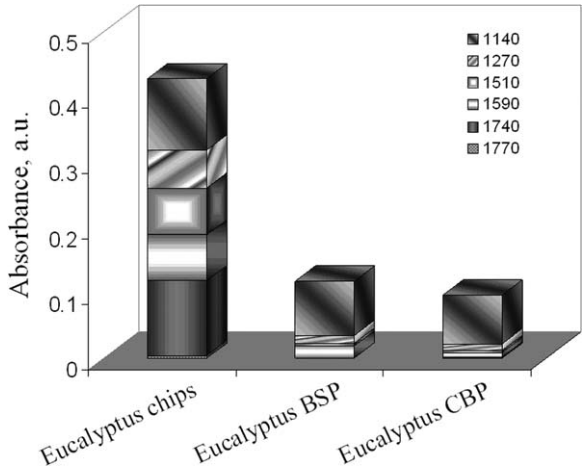

FIG. 5. The variations of the integral absorption of the representative lignin bands from the spectra of the eucalyptus samples.

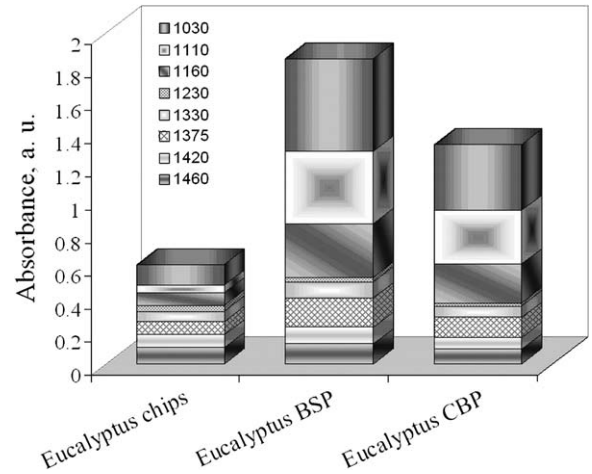

FIG. 7. The variations of the integral absorption of the common representative bands of lignin and cellulose from the spectra of the eucalyptus samples.

decrease in the pulp sample after chlorite bleaching. This means that after the chlorite bleaching process, lignin is partially removed.

Moreover, the integral absorption of the IR bands assigned to the characteristic bending or stretching of different groups from cellulose in pulp samples is higher than in the spectra of eucalyptus chips.

At the same time, the bands for the chlorite-bleached pulp sample are lower than those for the unbleached pulp sample. This means that the cellulose structure is somehow degraded after the bleaching process.

The integral absorption bands assigned to the characteristic bending or stretching groups common to lignin and cellulose show the same behavior as the bands assigned to the characteristic bending or stretching of different groups for cellulose (see Figs. 6 and 7).

The strongest variations of the integral absorptions are shown for the following bands: 1030 cm^{-1}, assigned to C_{alkyl}–O ether vibrations, $–OCH_3$, and β–O–4 in guaiacol and C–C and C–O stretching in cellulose I and cellulose II; 1110 cm^{-1}, assigned to the aromatic C–H in-plane deformation (typical for S units), secondary alcohols, C=O stretch, and ring asymmetric stretching in cellulose I and cellulose II; and 1160 cm^{-1}, assigned to the C–H in-plane deformation of the G ring and C–O–C asymmetric stretching in cellulose I and cellulose II.

The intensities of several IR absorption bands characteristic of cellulose were also compared to the intensity of the 1510 cm^{-1} band, which is sometimes used as an internal standard assigned to the benzene ring stretching of lignin (see Table V).

The relationship between lignin and carbohydrates can be calculated by the ratio of certain bands from the FT-IR spectra. The lignin/carbohydrate ratios are decreasing in the sample series studied, caused simultaneously by the decreasing of the 1510 cm^{-1} band and the decreasing of the carbohydrate-assigned bands. The variation of the lignin/carbohydrate ratio between samples is in good agreement with the ratio obtained from the data presented in Table I.

For a good characterization of the eucalyptus chip sample and the unbleached pulp samples, FT-IR spectra of the fractions obtained by successive extractions were analyzed. Figure 8 presents the "fingerprint" region of the FT-IR spectra of the acetone extractive for eucalyptus chips and unbleached brown stock pulp. By chemical determination, the amounts of acetone extractives in the samples are 1.40 wt % for the eucalyptus chip sample and 1.00 wt % for the unbleached eucalyptus BS sample. The differences, which appear in the IR spectra of the samples, are due to the fact that some extractives (resin acids, lignins, and triglycerides) investigated by gas chromatography–flame ionization detection (GC-FID) analysis are not detected or the detected amount is very low. Also, all determined extractive amounts are lower in the unbleached eucalyptus BS pulp sample than in the eucalyptus chip sample.[20]

The extractive spectra present some general differences in

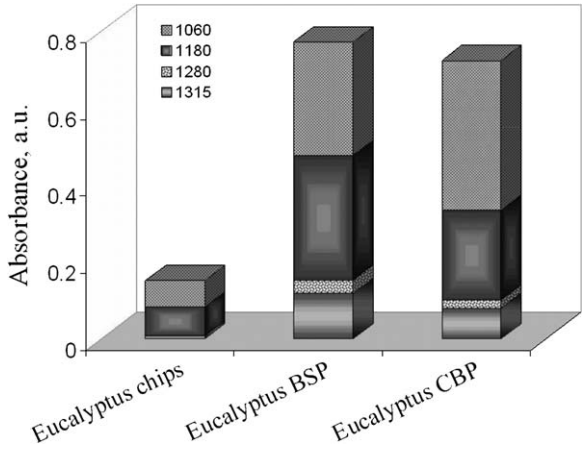

FIG. 6. The variations of the integral absorption of the representative cellulose bands from the spectra of the eucalyptus samples.

TABLE V. Lignin/carbohydrate ratio calculated from FT-IR spectra.

Sample	I_{1510}/I_{1375}	I_{1510}/I_{1158}	I_{1510}/I_{895}	L/C[a]
Eucalyptus chips	0.911	0.960	3.600	0.391
Eucalyptus BSP[b]	0.023	0.012	0.045	0.017
Eucalyptus CBP[c]	0.016	0.009	0.030	—

[a] Lignin/carbohydrate ratio, chemically determined; for L/C ratio the highest values of the total amount from Table I were used.
[b] BSP: brown stock pulp.
[c] CBP: chlorite-bleached pulp.

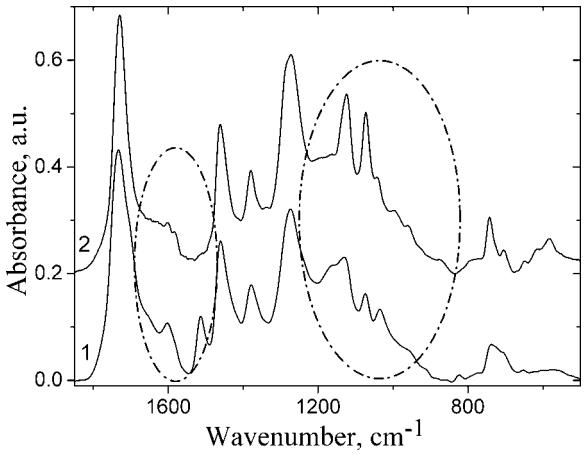

FIG. 8. FT-IR spectra of the acetone extractive samples: (*1*) eucalyptus chips, (*2*) eucalyptus brown stock pulp.

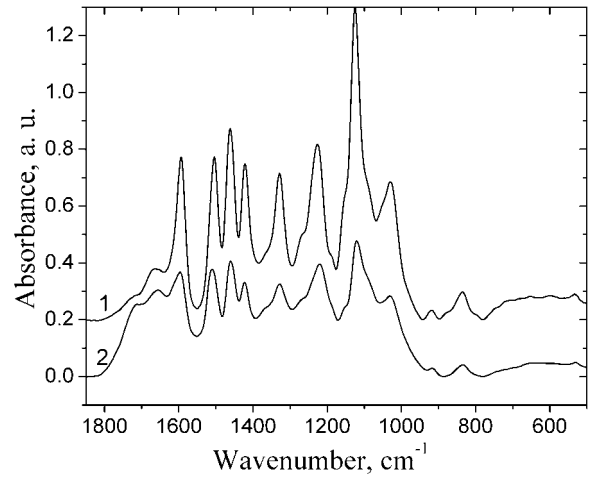

FIG. 9. FT-IR spectra of the lignin samples: (*1*) enzymatic mild acidolysis eucalyptus chips, (*2*) residual Kraft eucalyptus chips.

the 1650–1500 cm^{-1} and 1200–900 cm^{-1} regions. For example, in the eucalyptus chip spectrum, the band at 1653 cm^{-1}, assigned to water and associated with extractives, is shifted to 1640 cm^{-1} in the unbleached BS pulp sample. In the eucalyptus chip sample the band at 1587 cm^{-1}, assigned to C=O stretch and CH deformations, is more evident, and in the BS unbleached pulp sample this band is shifted to 1596 cm^{-1}. The band at 1510 cm^{-1}, assigned to C–H deformations, is evident in the normal spectra of eucalyptus chips, while in the unbleached BS pulp sample it was possible to detect this band only using the second-derivative spectra and deconvolution process. In the eucalyptus chip sample spectrum, the band at 1161 cm^{-1}, assigned to C–H in-plane deformations, is overlapped with the band at 1125 cm^{-1}, while in the unbleached BS pulp sample it was again only possible to detect this band using the second-derivative spectra and deconvolution process.

Also, the intensity of the band at 1072 cm^{-1}, assigned to C–O deformation in secondary alcohols and aliphatic ethers, is increasing in the unbleached BS pulp sample, while the band at 1040 cm^{-1}, assigned to C–C and C–O stretching, is present in the unbleached BS pulp sample as a shoulder. The integral absorptions of these bands were determined by the deconvolution process.

The band positions in the extractive spectra are overlapped with those assigned to different lignin or carbohydrate group vibrations. However, because of their low content, they will only influence the global FT-IR spectra to a small extent.

The FT-IR spectra of lignins obtained by enzymatic mild acidolysis and the residual Kraft of eucalyptus chips are presented in Fig. 9.

The FT-IR spectra of lignin samples show the bands assigned to the characteristic bending or stretching of different specific groups of lignin in the "fingerprint" region. The differences that appear in the spectra are due to the extraction method used. Generally, the extraction methods for lignin samples induce differences in the lignin structure. The integral absorption of the bands from residual Kraft lignin is lower than the integral absorption of the bands from enzymatic mild acidolysis lignin. Also, the separation of the bands is better in the case of the enzymatic mild acidolysis lignin. The integral absorption of the bands at 1595, 1510, 1455, 1422, 1330, 1220, 1120, and 1027 cm^{-1} is higher in enzymatic mild acidolysis eucalyptus chip lignin than in residual Kraft eucalyptus chip lignin.

Fourier transform infrared spectroscopy gives us important details about the characteristic structure of such complex samples as wood, pulp, cellulose, extractives, and lignin. Second-derivative spectra and the deconvolution process also play an important role. Using the spectral study, correlations

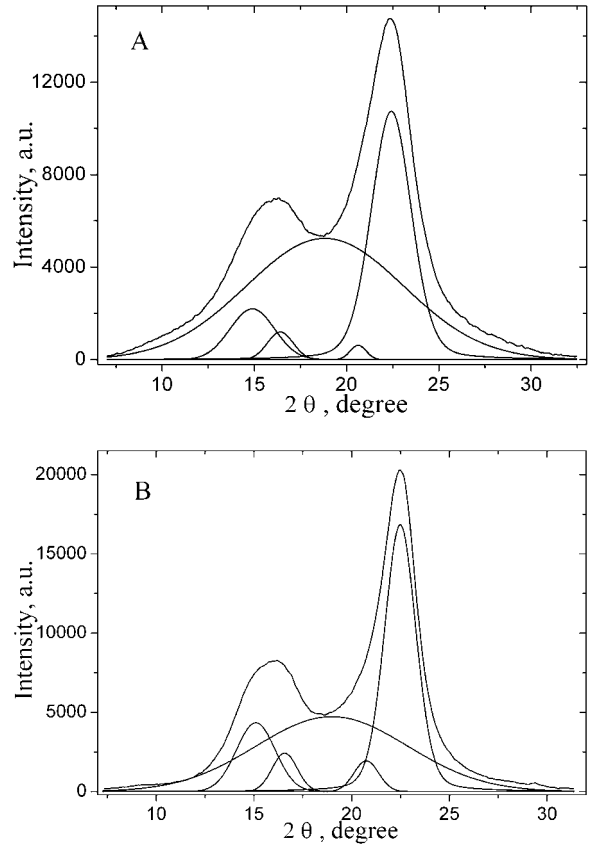

FIG. 10. Deconvoluted X-ray diffractograms of (**A**) eucalyptus chips and (**B**) eucalyptus brown stock pulp samples.

TABLE VI. The calculated values of several parameters estimated from the diffraction pattern for the samples studied.

Parameter[a]	Eucalyptus chips	Eucalyptus BSP
Cr.I.	0.423	0.543
Cr.I.′	0.501	0.690
L_{002} (nm)	2.383	3.504
X	0.272	0.455
O.I.	0.636	0.759
Mesomorphism	0.213	0.216
Cellulose content	0.603	0.978

[a] Cr.I.: Crystalline index; Cr.I.′: crystalline intensity index; L_{002}: apparent crystallite size for the 002 reflection; X: proportion of crystallite interior chains; O.I.: orientation index.

were made between wood composition and the energy of hydrogen bonds and hydrogen bonding distance and also between the integral absorptions of the bands and lignin content and the lignin/carbohydrate ratio.

X-ray Diffraction Results. Figure 10 shows the X-ray diffractograms of the *Eucalyptus globulus* and brown stock unbleached samples. The X-ray peaks at $2\theta = 15°$ and 16.5° merged into a broad band, which is consistent with the literature data.[42,43] The most prominent peak was $2\theta = 22.4°$, and it was used in our evaluations. This peak is assigned to the (200) plane, which is not parallel to any face. The X-ray diffraction pattern of wood is mainly that of cellulose.

In order to examine the intensities of the diffraction bands and to establish the crystalline and the amorphous areas more exactly, the diffractograms were deconvoluted using Gaussian and mixed Gaussian–Lorentzian profiles (Fig. 10).

The positions of the peaks of the cellulose crystalline form I[29] were found not to be significantly different in eucalyptus chips and brown stock unbleached pulp samples.

After deconvolution, five bands were observed, namely, the 15° (2θ) reflection assigned to the (101) crystallographic plane; the 16.5° (2θ) reflection, assigned to the ($10\bar{1}$) crystallographic plane; the 18.9° (2θ) reflection, assigned to amorphous phases; the 20.4° (2θ) reflection, assigned to the (012) crystallographic plane; and the 22.4° (2θ) reflection, assigned to the (002) or (200) crystallographic plane of cellulose I.[23–28,43,44] All peaks from the diffractograms are increasing in the pulp sample in comparison to the chip sample.

Crucial for the analysis of XRD data is the separation of the reflection (002) from the amorphous background and the reflections (012), (101), and ($10\bar{1}$).

In Table VI the calculated parameters for the studied samples are presented. The uncertainties in the crystallinity index determination are 3% ($N = 3$) and in the intensity ratio are 4%. All calculated values of the estimated parameters increase for the unbleached brown stock pulp as compared to the eucalyptus chip sample. The elimination of the hemicelluloses and lignin determines an increase in the crystallinity index. In unbleached pulp sample there is a large amount of cellulose, approximately 98%, and the diffraction pattern is not influenced by other components, while in the case of the chip sample, the lignin and hemicelluloses components are strongly present along with the cellulose, which can influence the X-ray diffraction pattern. The crystalline peaks are wider and less intense in eucalyptus chips because of the reduced quantity of cellulose, so that the values describing the crystalline phase are smaller.

CONCLUSION

Fourier transform infrared spectroscopy and X-ray diffraction studies produce evidence that pulping treatment leads to compositional changes in the principal components of wood, such as lignin and cellulose. The correlations between the intermolecular hydrogen bonding, hydrogen bonding distance, crystallinity index, apparent crystallite size, crystallite interior chains, orientation index, mesomorphism, and mass fraction of cellulose in wood and spectral characteristics have been established.

ACKNOWLEDGMENTS

This work was done under the COST E4l project: Analytical Tools with Applications for Wood and Pulping Chemistry (http://KCL.FI/COST/index.html).

1. J. J. Morrell, Int. Biodet. Biodeg. **49,** 253 (2002).
2. A. C. O'Sullivan, Cellulose **4,** 173 (1997).
3. R. H. Atalla, "Celluloses", in *Comprehensive Natural Products Chemistry*, D. Barton, K. Nakanishi, and O. Meth-Cohn, Eds., (Elsevier Science, Oxford, 1999), 1st ed., Chap. 3, p. 529.
4. C. Y. Liang and R. H. Marchessault, J. Polym. Sci. **37,** 385 (1959).
5. R. H. Atalla, Science (Washington, D.C.) **223,** 283 (1984).
6. K. K. Pandey, J. Appl. Polym. Sci. **71,** 1969 (1999).
7. F. Dadashian and W. A. Wilding, Text. Res. J. **71,** 7 (2001).
8. N. S. Hon, "Surface chemistry of oxidized wood", in *Cellulose and Wood Chemistry and Technology,* C. Schuerch, Ed. (John Wiley and Sons, New York, 1989), p. 1401.
9. S. B. Lee, J. Bogaard, and R. L. Feller, "Accelerated thermal degradation of pulp sheets: effect of beating and importance of humidity", in *Cellulose and Wood Chemistry and Technology. 10th Cellulose Conferences, Syracuse, New York, 1988*, C. Schuerch, Ed. (John Wiley and Sons, New York, 1989), p. 863.
10. R. Hori and J. Sugiyama, Carbohydr. Polym. **52,** 449 (2003).
11. K. Tashiro and M. Kobayashi, Polymer **32,** 1516 (1991).
12. J. Mann and H. J. Marrinan, Faraday Trans. **1,** 492 (1956).
13. H. Siesler, H. Krässig, F. Grass, K. Kratzl, and J. Derkosch, Makromol. Chem. **42,** 139 (1975).
14. Y. Nishiyama, A. Isogai, T. Okano, M. Müller, and H. Chanzy, Macromolecules **32,** 2078 (1999).
15. A. J. Michell, Carbohydr. Res. **197,** 53 (1990).
16. D. Fengel and M. Ludwig, Papier **45,** 45 (1991).
17. J. Sugiyama, J. Persson, and H. Chanzy, Macromolecules **24,** 2461 (1991).
18. B. Hinterstoisser, M. Akerholm, and L. Salmén, Carbohydr. Res. **334,** 27 (2001).
19. M. Wada, J. Sugiyama, and T. Okano, J. Appl. Polym. Sci. **49,** 1491 (1993).
20. S. Willfor, *Summary of results of WG3 on the joint analysis effort of eucalypt and spruce samples, Proceedings of the COST E41 meeting, Progress of the "COST Action E41 Joint Analysis effort" on Wood and Fiber Characterisation* (Grenoble, France, April 12–13, 2006).
21. J. Puls, *Summary of WG2 results, Proceedings of the COST E41 meeting, Progress of the "COST Action E41 Joint Analysis effort" on Wood and Fiber Characterisation* (Grenoble, France, April 12–13, 2006).
22. E. de Jong, *Compositional characterisation of wood and pulps: Summary WG1, Proceedings of the COST E41 meeting, Progress of the "COST Action E41 Joint Analysis effort" on Wood and Fiber Characterisation*, (Grenoble, France, April 12–13, 2006).
23. T. Heinze and T. Liebert, Prog. Polym. Sci. **26,** 1689 (2001).
24. Cr. I. Simionescu, M. Grigoras, A. Cernatescu-Asandei, and Gh. Rozmarin, *Wood chemistry from Romania – the poplar and the willow trees* (Romanian Academy, Bucharest, 1973), p. 107.
25. P. H. Hermans, J. J. Hermans, D. Vermaas, and A. J. Weidinger, J. Polym. Sci **3,** 1 (1947).
26. O. Ant-Wuorinen and O. A. Visapä, Paperi ja Puu **49,** 207 (1961).
27. A. M. Donald and O. M. Astley, www.ccp13.ac.uk/fdr/2001/html/pdf/print/19.pdf (accessed 18/08/2005).
28. X. Colom, F. Carrillo, F. Nogues, and P. Garriga, Polym. Degrad. Stab. **80,** 543 (2003).
29. "Wood", in *Encyclopedia of Polymer Science and Technology,* B. L. Browning, Ed. (John Wiley and Sons, New York, 1971), Chap. 15, p. 1.

30. A. U. Ferraz, J. Baeza, J. Rodrigues, and J. Freer, Biores. Technol. **74,** 201 (2000).
31. A. K. Moore and N. L. Owen, Appl. Spectrosc. Rev. **36,** 65 (2001).
32. K. K. Pandey and A. J. Pitman, Int. Biodet. Biodeg. **52,** 151 (2003).
33. B. Mohebby, Int. Biodet. Biodeg. **55,** 247 (2005).
34. M. Schwanninger, J. C. Rodrigues, H. Pereira, and B. Hinterstoisser, Vib. Spectrosc. **36,** 23 (2004).
35. B. Hinterstosser and L. Salmen, Vib. Spectrosc. **22,** 111 (2000).
36. T. Kondo, Cellulose **4,** 281 (1997).
37. L. J. Bellamy, *The Infrared Spectra of Complex Molecules* (Chapman and Hall, London, 1975), p. 108.
38. F. Carrillo, X. Colom, J. J. Suñol, and J. Saurina, Eur. Polym. J. **40,** 2229 (2004).
39. H. Struszczyk, J. Macromol. Sci., A **23,** 973 (1986).
40. G. C. Pimentel and C. H. Sederholm, J. Chem. Phys. **24,** 639 (1956).
41. C.-H. Wan and J.-F. Kuo, Liq. Cryst. **28,** 535 (2001).
42. R. H. Newman, Solid State Nucl. Magn. Res. **15,** 21 (1999).
43. N. E. Marcovich, M. M. Reboredo, and M. I. Aranguren, Thermochim. Acta **372,** 45 (2001).
44. Y. Cao and H. Tan, Enzyme Microbiol. Technol. **36,** 314 (2005).